Structures and Rearrangement Reactions of Oxaferretane (C_2H_4OFe): A Theoretical Approach *

Peter Swanstrøm and Karl Anker Jørgensen
Department of Chemistry, Aarhus University, DK-8000 Aarhus C, Denmark

The photochemical rearrangement reactions of oxaferretane (**3**) have been investigated using *ab initio* methods. The geometry and electronic structure of both the substrate and of the products, an oxoiron–ethylene π complex (**4**) and vinyliron hydroxide (**5**), have been determined. From calculations of the excited states of (**3**) and (**4**) a mechanism for the photochemical rearrangement reaction (**3**) ⟶ (**4**) ⟶ (**5**) is suggested. The results obtained are discussed in relation to other oxo-transfer reactions.

The field of transition metal-catalysed oxidations has been extensively developed in recent years.[1] Many attempts have been made both experimentally and theoretically to elucidate the mechanism for these oxidation reactions.[1,2] One such reaction which has received considerable attention is the oxidation of alkenes by oxometal complexes.[1a,b,d,2b,c,g,h,j,m,o–w] For the formation of *e.g.* epoxides from an alkene and an oxometal complex two types of intermediates are often considered:[1,2b,c,g,h,j,m,o–w] one is the interaction of the alkene with the oxygen in the oxometal complex, (**1**), and the other is addition of the alkene to the oxo–metal bond leading to a metallaoxacycle, (**2**).

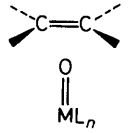

(**1**)

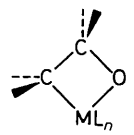

(**2**)

The metallaoxacycle (**2**) has been suggested as an alternative to (**1**) in the oxidation of alkenes by oxometal complexes, but according to our knowledge there is no direct evidence for it as an intermediate in oxidation reactions. Metallaoxacycles are on the other hand known to exist, *e.g.* [PtL_4] [L = $P(C_6H_5)_3$, $P(C_6H_4CH_3\text{-}p)_3$, or $As(C_6H_5)_3$] reacts with tetracyanoethylene oxide to give an oxaplatinetene complex which has been characterized by *X*-ray crystallographic investigations,[3] and oxatitanetane can be prepared by the addition of ketene to a titanium methylene complex or by the addition of a methylene fragment to a titanium ketene complex.[4]

Recently an oxaferretane, (**3**), has been observed by matrix-

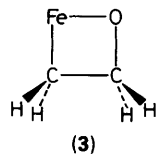

(**3**)

isolation Fourier-transform i.r. spectroscopy.[5] It was formed by a spontaneous insertion of atomic iron into the carbon–oxygen bond of ethylene oxide.[5] An oxaferretane complex has *e.g.* been suggested as the intermediate in the catalytic oxidation of alkenes by iron porphyrins.[2c,g,h,t–w] Visible photolysis of (**3**) leads to cleavage of the carbon–oxygen bond of the oxaferretane followed by formation of an oxoiron–ethylene π complex, (**4**).

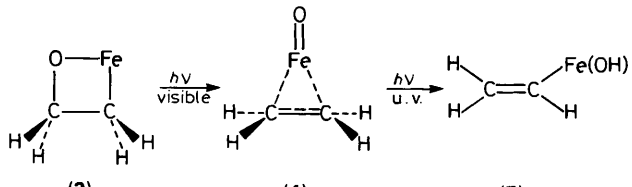

(**3**) (**4**) (**5**)

Scheme.

Further photolysis of (**4**) by u.v. light leads to activation of one of the C–H bonds in ethylene and formation of vinyliron hydroxide, (**5**). The reaction sequence is shown in the Scheme.

The purpose of the present study is to try to throw some light on the structures of (**3**)–(**5**) and the metathesis outlined in the Scheme in an attempt to understand these types of reactions and their relation to the involvement of these complexes in oxidation reactions. For these purposes *ab initio* calculations have been performed using the GAUSSIAN 86 program.[6]

Results and Discussion

The Geometrical Structures.—(*a*) *Oxaferretane*, (**3**). The structure of compound (**3**) has been optimized at a MP2/STO-3G* level of approximation and is shown below. It has been found that the most stable configuration has a planar ring structure and the electronic state is a quintet of *A'* symmetry.

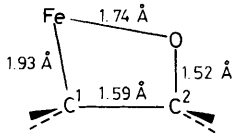

(**3**)

According to our knowledge no other oxaferretane structures have been characterized, whereas a few oxaplatinetane complexes are known, *e.g.* [$Pt\{C_2(CN)_4O\}\{As(C_6H_5)_3\}_2$], (**6**).[3b] Let us try to compare some of the structural data for (**3**) and (**6**). The carbon–carbon distances in the two systems are more or less identical, 1.59 in (**3**) and 1.58 Å in (**6**), whereas the carbon–oxygen distances differ somewhat, 1.52 in (**3**) and 1.36 Å in (**6**). The carbon–oxygen bond in compound (**3**) is slightly longer

* *Non-S.I. units employed:* Hartree (a.u.) ≈ 4.36×10^{-18} J, cal = 4.184 J.

than a normal carbon–oxygen bond (1.46 Å), whereas this bond is somewhat shorter in (**6**), and corresponds to the carbon–oxygen single bond in an aromatic system. The planar structure of (**3**) differs from that of (**6**) which is slightly distorted from planarity; this distortion has been interpreted in terms of minimization of the non-bonding interaction between the cyano groups attached to the carbons in the four-membered ring.[3b] The iron–carbon bond length in (**3**) matches other iron–carbon bond lengths found in mononuclear iron compounds with η-alkene ligands.[7a]

The total energy of the optimized structure of (**3**) is −1 400.6688 a.u. at a MP2/STO-3G* level of calculation. The insertion of atomic iron in the quintet state into the carbon–oxygen bond in ethylene oxide is exothermic by 150 kcal mol^{-1}. The triplet states of (**3**) are all less stable than the quintet A' ground state (see Table 1).

(*b*) *Oxoiron–ethylene π complex*, (**4**). Several attempts have been made to optimize the structure of compound (**4**). The lowest quintet state is unstable and it correlates with the lowest $^5A'$ state of (**3**). The lowest stable state of (**4**) is a triplet with C_{2v} symmetry ($^3B_1$). The energy, −1 400.6354 a.u., is lower than that of the lowest quintet by 0.0881 a.u. or 55 kcal mol^{-1}.

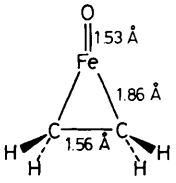

(**4**)

The oxoiron–ethylene π complex is an iron–η-alkene type of complex. The carbon–carbon and iron–carbon bond lengths are slightly longer and shorter, respectively, than those found in *e.g.* [Fe(CO)$_4$(η-alkene)] complexes.[7b] The oxo–iron bond length is slightly shorter than that reported for horseradish peroxidase.[8] The length of the carbon–carbon bond, 1.56 Å, indicates a complete absence of π character. Because of the close similarity to the work by Kafafi *et al.*[5] we shall, however, continue to use the nomenclature of their paper by calling (**4**) a π complex.

(*c*) *Vinyliron hydroxide*, (**5**). The MP2/STO-3G* optimized structure of compound (**5**) is shown below. It can be considered

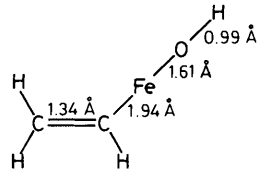

(**5**)

as an insertion of the iron–oxo fragment into one of the carbon–hydrogen bonds in ethylene. We have found that the iron–hydroxide fragment is linear; the iron–carbon and carbon–carbon bond lengths are in good agreement with those found in alkenyliron complexes.[7a] The iron–oxygen bond is relatively short compared with similar types of bonds found in other iron complexes, the reason being that the iron is both electronically and co-ordinatively unsaturated.

The total energy for (**5**) is −1 400.6776 a.u. and has been obtained for the system in a $^5A'$ state.

The Electronic Structures.—(*a*) *Compound* (**3**). Compound (**3**) can also be considered as being formed by an ethylene fragment and an oxoiron fragment (Fe=O). The bonding in its lowest electronic $^5A'$ state can be given a simple interpretation in terms of interaction between the highest occupied molecular orbital (h.o.m.o.) of ethylene and one of the singly occupied molecular orbitals (s.o.m.o.s) of π symmetry of oxoiron in its quintet state (FeO has six *d* electrons at Fe, two lone pairs at O, and the remaining four valence electrons allocated to one doubly occupied σ orbital and two singly occupied π orbitals). The interaction is shown schematically in (**A**).

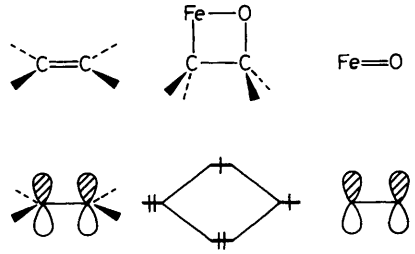

(**A**)

The lowest energy at a MP2/STO-3G* level of approximation for the quintet state of the oxoiron has been calculated to −1 323.3756 a.u. at an iron–oxygen bond distance of 1.60 Å, and the hypothetical formation of compound (**3**) from quintet oxoiron and ethylene becomes exothermic by 52 kcal mol^{-1}. The approximate distribution of the atomic spin population in the quintet state of the oxoiron fragment is illustrated in (**B**). At the iron atom there are approximately five unpaired electrons with α spin and at the oxygen atom there is approximately one

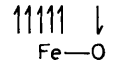

(**B**)

electron with a β spin. By using one α electron at iron and the β electron at oxygen in a simple spin-pairing picture with the two electrons located in the π orbital of ethylene we obtain the quintet state of compound (**3**). The calculated atomic spin populations are shown in parentheses in (**C**). The delocalization of atomic spin population from Fe to C supports the interpretation given above.

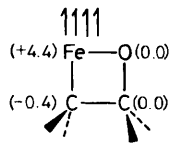

(**C**)

(*b*) *Compound* (**4**). Compound (**4**) can be formed by rearrangement of (**3**) by cleavage of the carbon–oxygen bond followed by a bidentate co-ordination of iron in the oxoiron fragment to the ethylene fragment.

We consider complex (**4**) to consist of two weakly interacting molecules, oxoiron in its triplet state and ethylene. The bonding between the two molecular fragments is established as shown below.

The interaction between the unoccupied 4*sp* hybrid orbital at iron and the occupied π orbital provides a stabilization of the π-electron pair, (**D**). The Mulliken overlap population of this interaction is calculated to be 0.24. Another interesting interaction is established between the empty 4p_x (Fe) and the empty ethylene π* orbitals. The molecular orbital (**E**) resulting from this interaction becomes so stabilized that it drops below the atomic 3*d* levels of Fe. Therefore two of the four unpaired 3*d* electrons are paired up in (**E**) with an overlap population of

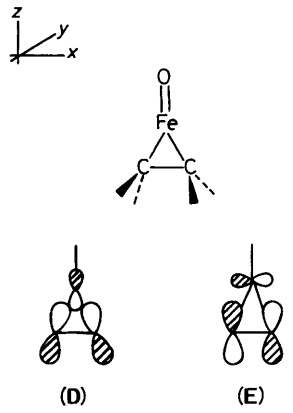

(D) (E)

0.07. At the same time Fe is oxidized; its atomic net charge increases from 0.18 (FeO) to 0.30 (C_2H_4FeO). This explains why complex (**4**) is more stable as a triplet than as a quintet.

The transfer of electrons from the iron *d* orbitals to the bonding orbital is consistent with the calculated atomic spin population of compound (**4**) as shown in (**F**).

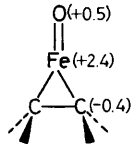

(F)

The $2p_y$ orbital at oxygen interacts with both the $4p_y$ orbital (**G**) and the diffuse d^* orbitals at iron (**H**). A total π_{yz}-overlap population of 0.14 is found. The same kind of interaction is found in the *xz* plane with a π_{xz}-overlap population of 0.16. The total π-overlap population between iron and oxygen thus becomes 0.30. With a total overlap population of 0.46 we are left

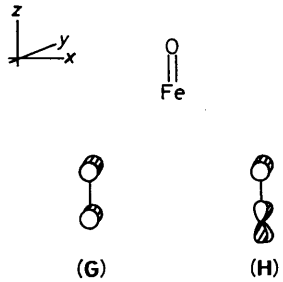

(G) (H)

with a σ-overlap population of 0.16. For comparison we have calculated the overlap populations of triplet FeO at the same internuclear distance, finding the π-overlap population to be 0.26 and the σ-overlap population to be 0.08. The attachment to ethylene has thus enhanced the stability of triplet FeO. In fact the total overlap population is increased from 0.34 (FeO) to 0.46 in (**4**).

(*c*) *Compound* (**5**). The third compound in the series, (**5**), also has a ground electronic state of $^5A'$, which might indicate that (**5**) is formed by insertion of quintet iron oxide into the carbon–hydrogen bond. Most remarkable is the linearity of the C–Fe–O–H fragment.

The carbon–carbon double bond in ethylene (π-overlap population 0.19) loses some of its π character by the insertion of quintet oxoiron into the carbon–hydrogen bond. The π-overlap population of the C=C bond actually decreases to 0.14, but this does not affect the bond distance to any significant extent. Let us thus focus attention on the linearity of the C–Fe–O–H fragment. The bonding between carbon and iron is essentially of σ character. The main bonding between iron and oxygen is also of σ character, leaving two lone-pair electrons at oxygen; these are of p_y and p_z character, respectively, as shown in (**I**) and (**J**). The

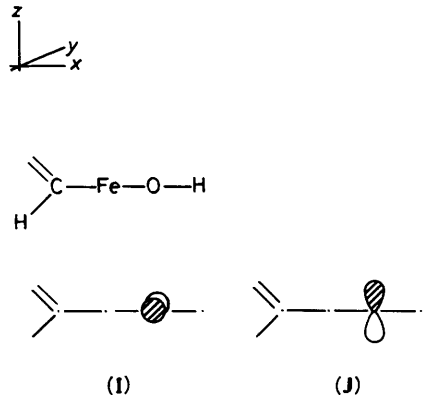

(I) (J)

four unpaired electrons at iron are allocated to four *d* orbitals, leaving the 4*p* orbitals at iron empty. Two of these 4*p* orbitals, $4p_y$ and $4p_z$, have the right symmetry to act as acceptor orbitals for electron density from the lone-pair electrons located at oxygen, and it is found that this type of back donation from oxygen to iron takes place in (**5**). This leads to an orbital picture for the iron–oxygen bond as shown in (**K**)—(**M**), where the

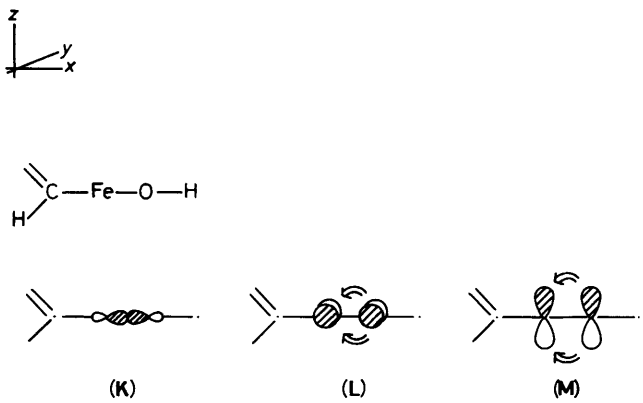

(K) (L) (M)

arrows show the flow of electron density. The π back donation as depicted leaves a sp_x hybrid orbital at oxygen available for interaction with the *s* orbital at hydrogen which extends the linearity to include hydrogen.

Computation.—As mentioned above, all computations reported in this paper were performed with the GAUSSIAN 86 program.[6]

The STO-3G* basis set employed is the one implemented in the program. It consists of the ordinary STO-3G basis for all the atoms, augmented with an extra set of five *d* functions for iron (exponent 0.39). Due to their diffuseness these additional *d* functions provide flexibility to the iron valence shell. We tested the two basis sets STO-3G and STO-3G* against each other for the FeO molecule in a quintet state. While computations with the smaller STO-3G basis did not converge at all, the larger STO-3G* led to the anticipated occupancy of the valence *d* shell of Fe, which turned out to have a gross orbital population of 4.9 α and 1.1 β electrons.

The anticipated accuracy of the bond lengths involving iron is poor, though presumably better than with a simple STO-3G basis. With the STO-3G basis, metal–carbon bond distances

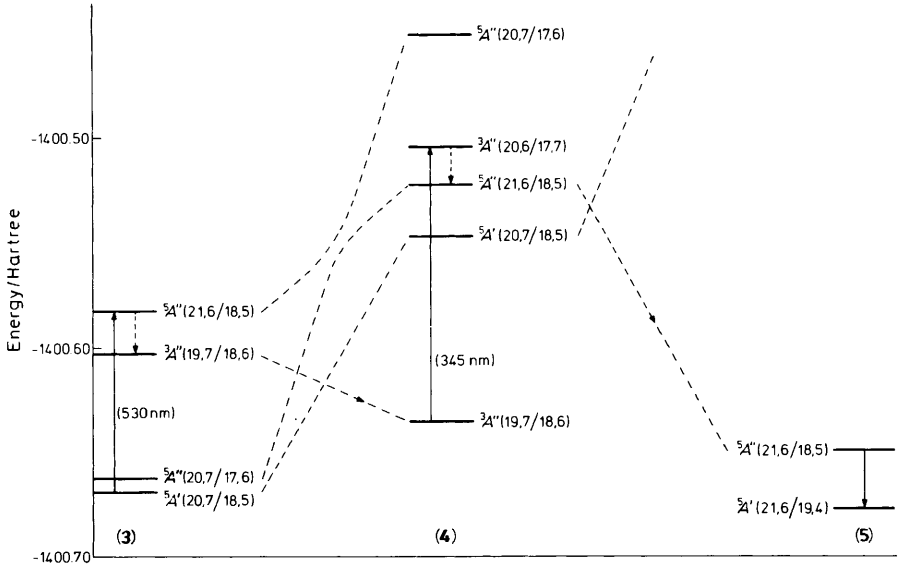

Figure. Correlation diagram for the lower electronic states of compounds (**3**)—(**5**). The vertical axis represents spin-projected Møller– Plesset second-order energies obtained with the STO-3G* basis discussed. The arrows indicate the suggested photochemical pathway (**3**) ⟶ (**4**) ⟶ (**5**). Possible intersystem crossings between nearly degenerate vibronic states of different spin multiplicity are indicated with dotted arrows pointing downwards

Table 1. Computed absolute energies (in Hartree) at the unrestricted Hartree–Fock (HF) and the projected Møller–Plesset (PMP2) levels for each of the species (**3**)—(**5**) in their lowest electronic states. The HF average value of the S^2 operator is also given for each state. The terminology $^5A'$ (20,7/18,5), say, refers to a $^5A'$ state based on an unrestricted Hartree–Fock wavefunction with $20a' + 7a''$ α-spin orbitals and $18a' + 5a''$ β-spin orbitals

Compd.	State	$\langle S^2 \rangle$	E(HF)	E(PMP2)	
(**3**)	$^5A''$ (21,6/18,5)	6.02	−1 400.3266	−1 400.5830	
	$^3A''$ (19,7/18,6)	2.02	−1 400.2858	−1 400.6030	
	$^5A''$ (20,7/17,6)	6.00	−1 400.3661	−1 400.6625	
	$^5A'$ (20,7/18,5)	6.00	−1 400.3667	−1 400.6688	Stable
(**4**)	$^5A''$ (20,7/17,6)	6.02	−1 400.1599	−1 400.4516	
	$^3A''$ (20,6/17,7)	2.75	−1 400.1813	−1 400.5050	
	$^5A''$ (21,6/18,5)	6.03	−1 400.2322	−1 400.5232	
	$^3A''$ (19,7/18,6)	2.75	−1 400.2876	−1 400.6354	Stable
(**5**)	$^5A''$ (21,6/18,5)	6.01	−1 400.3675	−1 400.6493	
	$^5A'$ (21,6/19,4)	6.03	−1 400.3795	−1 400.6776	Stable

(metal = Cr, Mn, or Fe) for metal carbonyls are typically 0.1—0.2 Å in error, while the bond lengths not involving the metal atom have an accuracy of 0.1 Å or better.[9] We expect the STO-3G* basis to perform better than the STO-3G for the bonds involving Fe. Although the lack of accuracy will certainly be reflected in the excitation energies, we are convinced that the nature of the suggested reaction mechanism will not change when a larger basis set calculation is performed.

The energy procedure used is unrestricted Hartree–Fock plus second-order Møller–Plesset correlation. Contaminations of the wavefunction due to unwanted spin components were annihilated using a projection technique due to Schlegel.[10] This procedure is referred to as projected MP2, or PMP2.

Geometry optimizations were done with respect to all bond distances and angles using the Berny method implemented in GAUSSIAN 86. The resulting geometries were not much different from the ones obtained using ordinary unrestricted Hartree–Fock gradients. The stability of the local minima was carefully examined. For compounds (**3**) and (**5**) the lowest stable electronic states were identified as quintets while the lowest stable electronic state of (**4**) appears to be a triplet. The corresponding stable geometries reported above were used to calculate a few of the vertically excited states of the three species, thus assuming an adiabatic approach. We have also calculated the lowest triplet of (**3**) and the three lowest quintets of (**4**) at the stable geometries. Although (**4**) is found to have C_{2v} symmetry we have reported all symmetry labels in the common C_s group, in order to facilitate drawing of the state correlation in the Figure.

Table 1 gives, for each of the three species in their lowest electronic states, the computed absolute energies (in Hartree) at the unrestricted Hartree–Fock (HF) and the projected Møller–Plesset (PMP2) levels. As a criterion for the purity of the spin state we also give the HF average value of the S^2 operator. The states given in the table have been carefully selected from a large number of systematically generated electronic states.

Rearrangement Reactions of Oxaferretane.—In this section we offer a description of the possible photochemical pathways connecting oxaferretane (**3**) with the oxoiron–ethylene π complex (**4**) and vinyliron hydroxide (**5**). We stress that this attempt can be no more complete than the available information about the excited states of the three compounds.

The Figure displays some of the lowest electronic states of the three compounds. The most important correlations are indicated together with an avoided crossing. The vertical axis represents spin-projected Møller–Plesset second-order energies obtained with the STO-3G* basis mentioned in the previous section. Each *d* shell was spanned by five *d* functions.

The ground states of compounds (**3**) and (**5**) are both of $^5A'$ symmetry. For (**4**) the lowest state is of $^3A''$ symmetry. The lowest quintet state of (**4**) is unstable and correlates with the ground state of (**3**). Due to the near degeneracy between the lowest $^3A''$ state and one of the excited $^5A''$ states of (**3**) we anticipate strong spin–orbit coupling between the vibronic levels of the two states. Hence photoexcited oxaferretane molecules could spill from the $^5A''$ into the $^3A''$ state, resulting in production of the π complex (**4**). The photoexcitation threshold is calculated to be approximately 530 nm, in agreement with the observations made by Kafafi *et al.*[5]

Table 2 contains the calculated overlap populations of the

Table 2. Overlap populations of the electronic states involved in the photochemical pathway (3) ⟶ (4) ⟶ (5)

Compd.	State	Fe–O	Fe–C	C–C
(3)	$^5A'$ (20,7/18,5)	0.275	0.233	0.346
	$^5A''$ (21,6/18,5)	0.111	0.290	0.341
	$^3A''$ (19,7/18,6)	0.274	0.270	0.352
(4)	$^3A''$ (19,7/18,6)	0.368	0.171	0.380
	$^3A''$ (20,6/17,7)	0.305	0.168	0.386
	$^5A''$ (21,6/18,5)	0.267	0.225	0.361
(5)	$^5A''$ (21,6/18,5)	0.392	0.370	0.539
	$^5A'$ (21,6/19,4)	0.394	0.365	0.540

three states involved in the photoexcitation of compound (3). The initial step ($^5A' \longrightarrow {}^5A''$) is characterized by a near rupture of the Fe–O bond and a moderate increase of the Fe–C overlap population. The intersystem crossing ($^5A'' \longrightarrow {}^3A''$), however, restores the Fe–O overlap population to its ground-state value and adjusts moderately the Fe–C and C–C values. The net result of the intersystem crossing is a reinforcement of the Fe–C–C framework relative to the Fe–O fragment. The subsequent rearrangement of (3) $^3A''$ to (4) $^3A''$ results in a weakening of the Fe–C and a strengthening of the Fe–O bonds.

Due to its stability the π complex may remain forever trapped as a triplet until it is stimulated by photons. Because of the near degeneracy between the lowest $^5A''$ and one of the excited $^3A''$ states we again anticipate strong spin–orbit coupling between the vibronic levels of the two states. Photoexcited molecules of the complex (4) may thus spill from $^3A''$ into $^5A''$ leading to the production of vinyliron hydroxide (5), as indicated in the Figure. We note that compound (3) may be regenerated concurrently as a result of this process. The photoexcitation threshold is calculated to be approximately 345 nm, in agreement with that reported by Kafafi *et al.*[5] It also appears from Table 2 that the net result of the photoexcitations of (4) ($^3A'' \longrightarrow {}^3A'' \longrightarrow {}^5A''$) is a lowering of the Fe–O and an increase of the Fe–C overlap population. When rearranging from (4) $^5A''$ to (5) $^5A''$ (or A') all the three overlap populations are increased substantially. In particular, the large C–C value indicates that we are in fact dealing with a vinyl fragment.

The reaction sequence shown in the Scheme is closely related to the discussion of the involvement of metallaoxacycles in metal-centred oxo-transfer reactions. The first step, the insertion of atomic iron into the carbon–oxygen bond in ethylene oxide, has also been observed when [PtL_4] [L = $P(C_6H_5)_3$, $P(C_6H_4CH_3\text{-}p)_3$, or $As(C_6H_5)_3$], a d^{10} complex, reacts with tetracyanoethylene oxide.[3] Both reactions are in principle of the opposite type of the one suggested for the formation of ethylene oxide from metallaoxacycles. The second step in the Scheme leads to an oxoiron–η-alkene type of complex. According to our knowledge there are only few other types of complexes known which contain an oxo–metal bond and a co-ordinated alkene.[11] One such complex was obtained by reaction of ethylene oxide and [$WCl_2(PMePh_2)_4$] and is shown below.

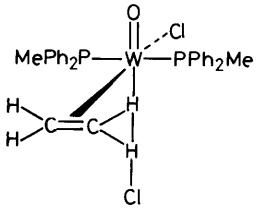

(7)

This reaction which is an oxidative addition is in principle of the same type as the second step in the Scheme, but there are two differences between the two reactions: (*i*) the reaction step in the Scheme needs photons to take place, whereas this is not the case for the formation of (7); (*ii*) the formation of (4) in the Scheme is indicated to take place *via* (3), whereas there are both experimental[12] and theoretical[13] indications that the reaction of ethylene oxide and [$WCl_2(PMePh_2)_4$] takes place as an attack of the oxygen in ethylene oxide on an empty orbital at tungsten in [$WCl_2PMePh_2)_3$] leading to an oxygen abstraction followed by co-ordination of ethylene. The oxygen abstraction from ethylene oxide is caused by a two-electron transfer from tungsten into the σ^*_{C-O} antibonding molecular orbital in ethylene oxide.[13] The reverse type of reaction, addition of alkenes to the oxo ligands in high-valent oxometal complexes, has been suggested to take place *via* the reverse type of electron transfer.[2i]

The photochemical rearrangement outlined in the Figure might thus not be the only mechanism for the formation of the different species; the reaction may have some relation to the interaction between an alkene and an oxometal system as shown in (1) and (2). The first step in the reaction between atomic iron and ethylene oxide might then be oxygen abstraction from ethylene oxide by the iron atom leading to ethylene and iron oxide. The three products can then be regarded as resulting from three different ways of trapping iron oxide by ethylene.

Conclusion

Three iron compounds, oxaferretane (3), oxoiron–ethylene π complex (4), and vinyliron hydroxide (5), have been investigated theoretically. Geometry optimizations have verified that (3) and (5) are planar molecules with $^5A'$ ground states, while (4) has C_{2v} symmetry and a $^3A''$ ground state. The photochemistry of the three compounds has been described by Kafafi *et al.*[5] and we have discussed the mechanisms associated with the photochemical reactions connecting the compounds. We suggest that the rearrangement (3) ⟶ (4) involves a quintet ⟶ triplet intersystem crossing and a trapping of the π complex in a $^3A''$ state. Subsequent photostimulation of (4) leads to (5), probably *via* a triplet ⟶ quintet intersystem crossing. Our conclusions are in agreement with the experimental observations made by Kafafi *et al.*[5]

Acknowledgements

The computations reported were made possible through a grant from the Danish Natural Science Research Council.

References

1 See, for example, (*a*) R. A. Sheldon and J. K. Kochi, 'Metal-Catalyzed Oxidations of Organic Compounds,' Academic Press, New York, 1981; (*b*) B. Meunier, *Bull. Soc. Chim. Fr.*, 1983, 345; 1986, 578; (*c*) R. H. Holm, *Chem. Rev.*, 1987, **87**, 1401; (*d*) K. A. Jørgensen, *ibid.*, 1989, **89**, 431.

2 See, for example, (*a*) A. O. Chong and K. B. Sharpless, *J. Org. Chem.*, 1977, **42**, 1587; (*b*) F. Freeman, *Chem. Rev.*, 1975, **75**, 439; (*c*) K. B. Sharpless, A. Y. Teranishi, and J. E. Bäckvall, *J. Am. Chem. Soc.*, 1977, **99**, 3120; (*d*) H. Mimoun, *J. Mol. Catal.*, 1980, **7**, 1; (*e*) M. G. Fron and K. B. Sharpless, in 'Asymmetric Synthesis,' ed. J. D. Morrison, Academic Press, New York, 1986, vol. 5, 193; (*f*) R. D. Bach, G. J. Wolber, and B. A. Coddens, *J. Am. Chem. Soc.*, 1984, **106**, 6098; (*g*) A. K. Rappé and W. A. Goddard, III, *ibid.*, 1982, **104**, 3287; (*h*) K. Yamaguchi, Y. Takahara, and T. Fueno, in 'Applied Quantum Chemistry,' eds. V. H. Smith, H. F. Schaefer III, and K. Morukuma, D. Reidel, Dordrecht, 1986, p. 155; (*i*) K. A. Jørgensen and R. Hoffmann, *J. Am. Chem. Soc.*, 1986, **108**, 1867; (*j*) *ibid.*, 1987, **109**, 698; (*k*) K. A. Jørgensen and R. Hoffmann, *Acta Chem. Scand., Ser.*

B, 1986, **40**, 411; (*l*) K. A. Jørgensen, R. A. Wheeler, and R. Hoffmann, *J. Am. Chem. Soc.*, 1987, **109**, 3240; (*m*) E. G. Samsel, K. Srinivasan, and J. K. Kochi, *ibid.*, 1985, **107**, 7606; (*n*) K. F. Purcell, *Organometallics*, 1985, **4**, 509; (*o*) J. T. Groves, W. J. Kruper, and R. C. Haushalter, *J. Am. Chem. Soc.*, 1980, **102**, 6375; (*p*) M-E. De Carvalho and B. Meunier, *Tetrahedron Lett.*, 1983, **24**, 3621; (*q*) J. P. Collman, J. I. Brauman, B. Meunier, T. Hayashi, T. Kodadek, and S. A. Raybuck, *J. Am. Chem. Soc.*, 1985, **107**, 2000; (*r*) J. T. Groves and M. K. Stern, *ibid.*, 1987, **109**, 3812; (*s*) J. T. Groves and T. E. Nemo, *ibid.*, 1983, **105**, 5786; (*t*) J. P. Collman, T. Kodadek, and J. T. Brauman, *ibid.*, 1986, **108**, 2588; (*u*) J. T. Groves and Y. Watanabe, *ibid.*, p. 507; (*v*) A. Sevier and M. Fontecare, *ibid.*, p. 158; (*w*) J. T. Groves, G. E. Avaria-Neisser, K. M. Fish, M. Imachi, and R. L. Kuckowsky, *ibid.*, p. 3837; (*x*) J. T. Groves, R. C. Haushalter, M. Nakamura, T. E. Nemo, and B. Evans, *ibid.*, 1981, **103**, 2884.

3 (*a*) J. A. Ibers, *Chem. Soc. Rev.*, 1982, **11**, 57; (*b*) R. Schlodder, J. A. Ibers, M. Lenarda, and M. Graziani, *J. Am. Chem. Soc.*, 1974, **96**, 6893.

4 S. C. Ho, S. Hentges, and R. H. Grubbs, *Organometallics*, 1988, **7**, 780.

5 Z. H. Kafafi, R. H. Hauge, W. E. Billups, and J. L. Margrave, *J. Am. Chem. Soc.*, 1987, **109**, 4775.

6 M. J. Frisch, J. S. Binkley, H. B. Schlegel, K. Raghavachari, C. F. Melius, R. L. Martin, J. J. P. Stewart, F. W. Bobrowicz, C. M. Rohlfing, L. R. Kahn, D. J. Defrees, R. Seeger, R. A. Whiteside, D. J. Fox, E. M. Fleuder, and J. A. Pople, GAUSSIAN 86, Carnegie-Mellon Quantum Chemistry Publishing Unit, Pittsburgh, Pennsylvania, 1984.

7 (*a*) M. D. Johnson, in 'Comprehensive Organometallic Chemistry,' eds. G. Wilkinson, F. G. A. Stone, and E. W. Abel, Pergamon, Oxford, 1982, vol. 4, p. 331; (*b*) A. J. Deeming, in *ibid.*, p. 377.

8 J. E. Penner-Hahn, K. S. Eble, T. J. McMurry, M. Renner, A. L. Balch, J. T. Groves, J. H. Dawson, and K. O. Hodgson, *J. Am. Chem. Soc.*, 1986, **108**, 7819.

9 W. J. Hehre, L. Radom, P. von R. Schleyer, and J. A. Pople, 'Ab Initio Molecular Orbital Theory,' Wiley, New York, 1986.

10 H. B. Schlegel, *J. Chem. Phys.*, 1986, **84**, 4530.

11 J. C. Bryan, S. J. Geib, A. L. Rheingold, and J. L. Mayer, *J. Am. Chem. Soc.*, 1987, **109**, 2826.

12 J. L. Mayer, personal communication.

13 B. Schiøtt and K. A. Jørgensen, *J. Chem. Soc., Daltan Trans.*, 1989, 2009.

Received 11*th July* 1989; *Paper* 9/02936B